ESM Figure 1

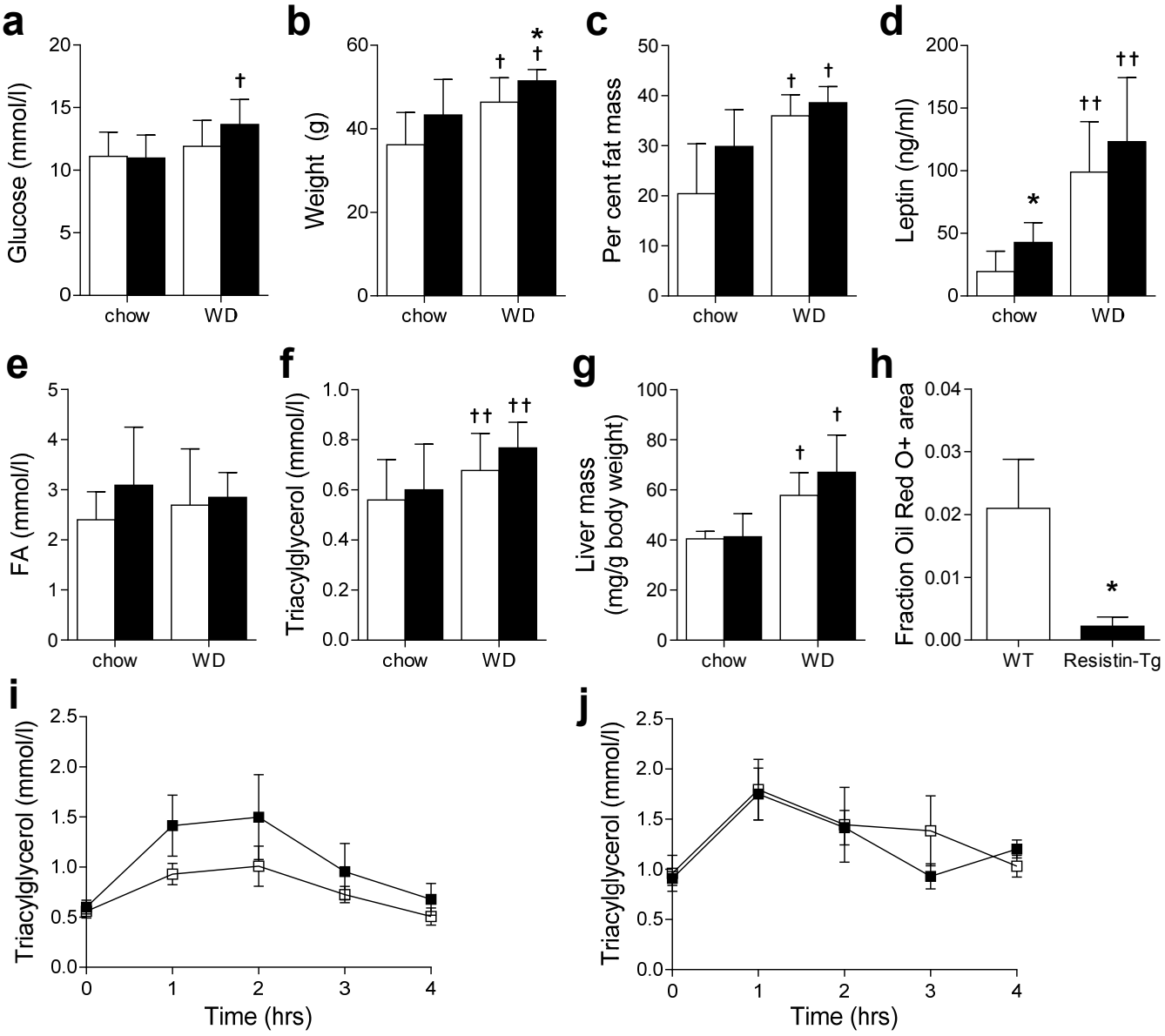
a
Glucose (mmol/l)
chow
WD
b
Weight (g)
c
Per cent fat mass
d
Leptin (ng/ml)
e
FA (mmol/l)
f
Triacylglycerol (mmol/l)
g
Liver mass (mg/g body weight)
h
Fraction Oil Red O+ area
WT
Resistin-Tg
i
Triacylglycerol (mmol/l)
Time (hrs)
j
Triacylglycerol (mmol/l)
Time (hrs)

ESM Figure 2

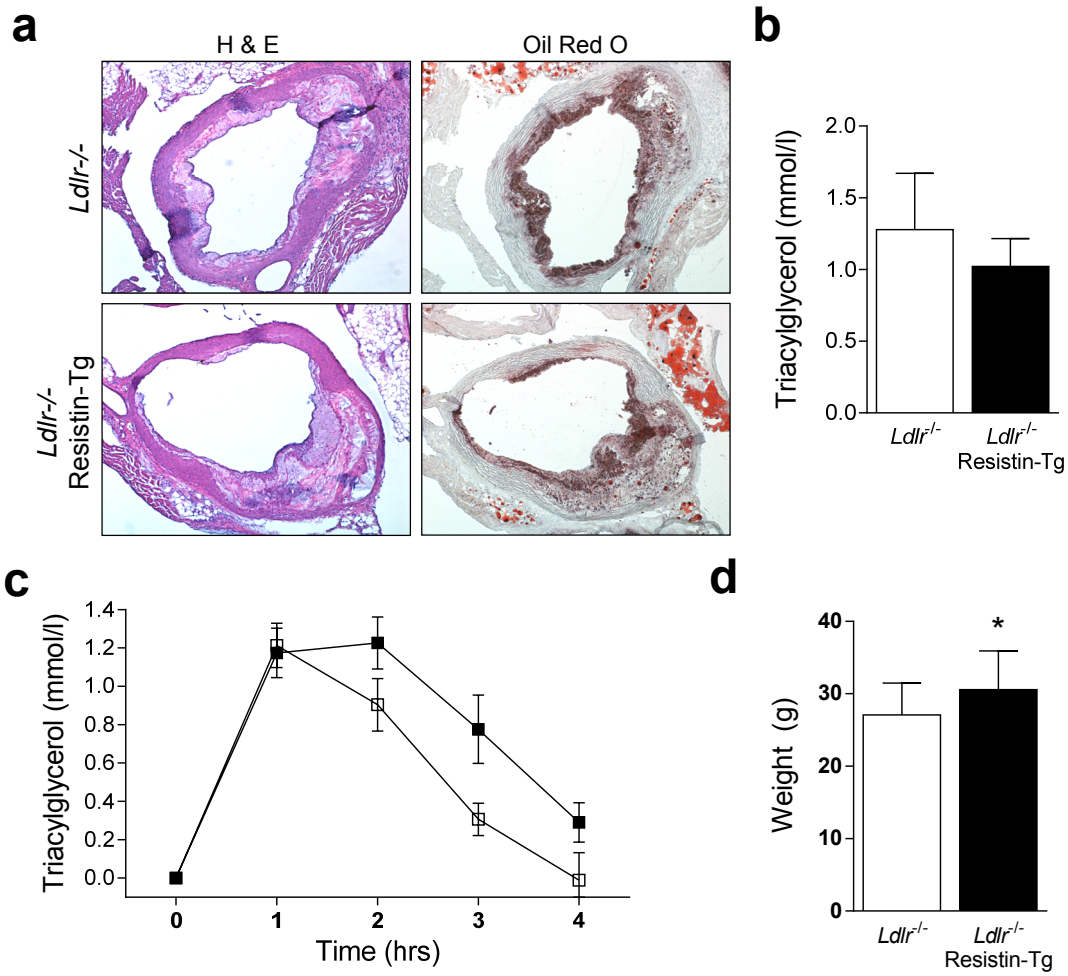
a
H & E
Oil Red O
Ldlr-/-
Ldlr-/-
Resistin-Tg
b
Triacylglycerol (mmol/l)
2.0
1.5
1.0
0.5
0.0
Ldlr-/-
Ldlr-/-
Resistin-Tg
c
Triacylglycerol (mmol/l)
1.4
1.2
1.0
0.8
0.6
0.4
0.2
0.0
0
1
2
3
4
Time (hrs)
d
Weight (g)
40
30
20
10
0
*
Ldlr-/-
Ldlr-/-
Resistin-Tg

ESM Figure 3

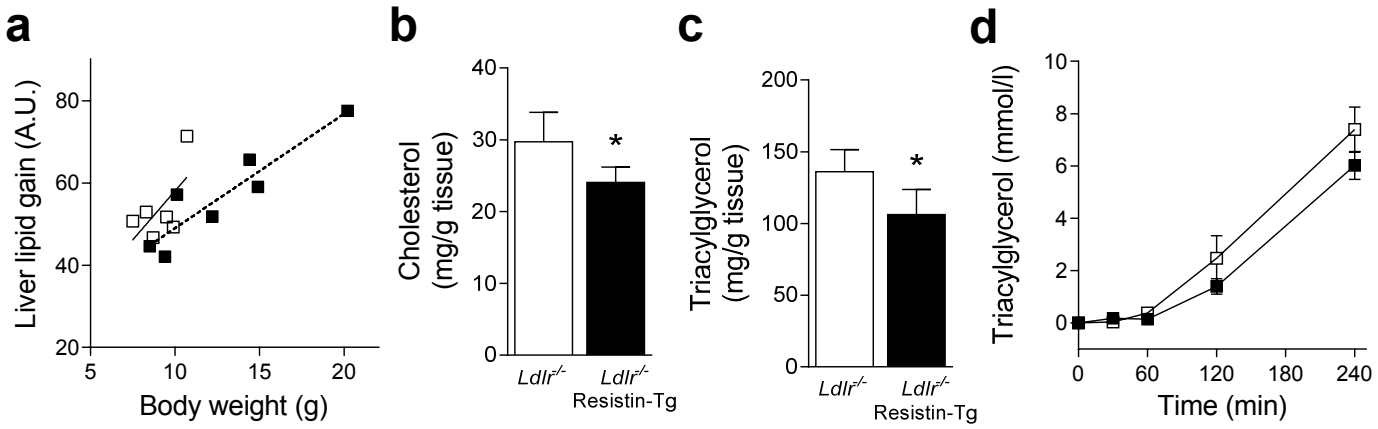
a
Liver lipid gain (A.U.)
Body weight (g)
b
Cholesterol (mg/g tissue)
Ldlr-/-
Ldlr-/- Resistin-Tg
c
Triacylglycerol (mg/g tissue)
Ldlr-/-
Ldlr-/- Resistin-Tg
d
Triacylglycerol (mmol/l)
Time (min)

ESM Figure 4

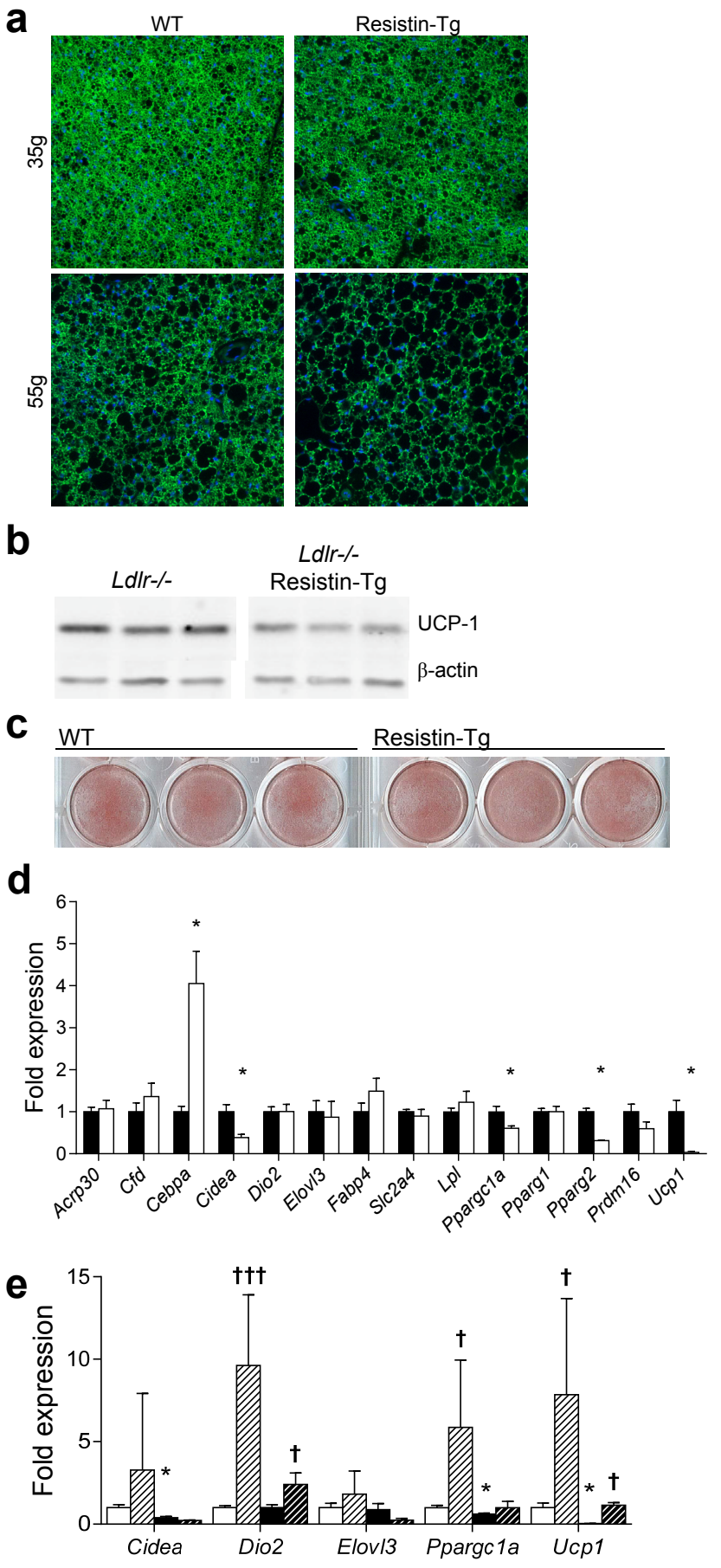
a
WT
Resistin-Tg
35g
55g
b
Ldlr-/-
Ldlr-/-
Resistin-Tg
UCP-1
β-actin
c
WT
Resistin-Tg
d
Fold expression
Acrp30
Cfd
Cebpa
Cidea
Dio2
Elovl3
Fabp4
Slc2a4
Lpl
Ppargc1a
Pparg1
Pparg2
Prdm16
Ucp1
e
Fold expression
Cidea
Dio2
Elovl3
Ppargc1a
Ucp1

ESM Figure 5

a

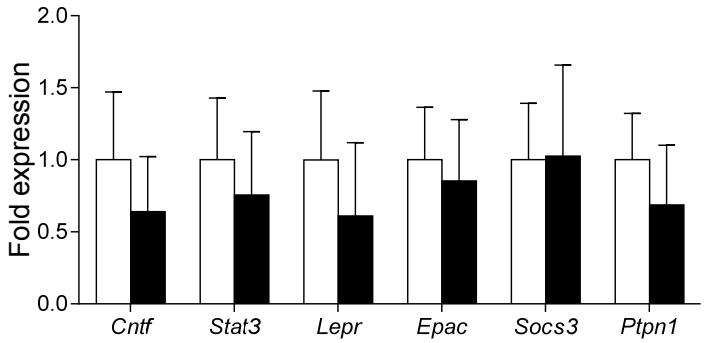

b

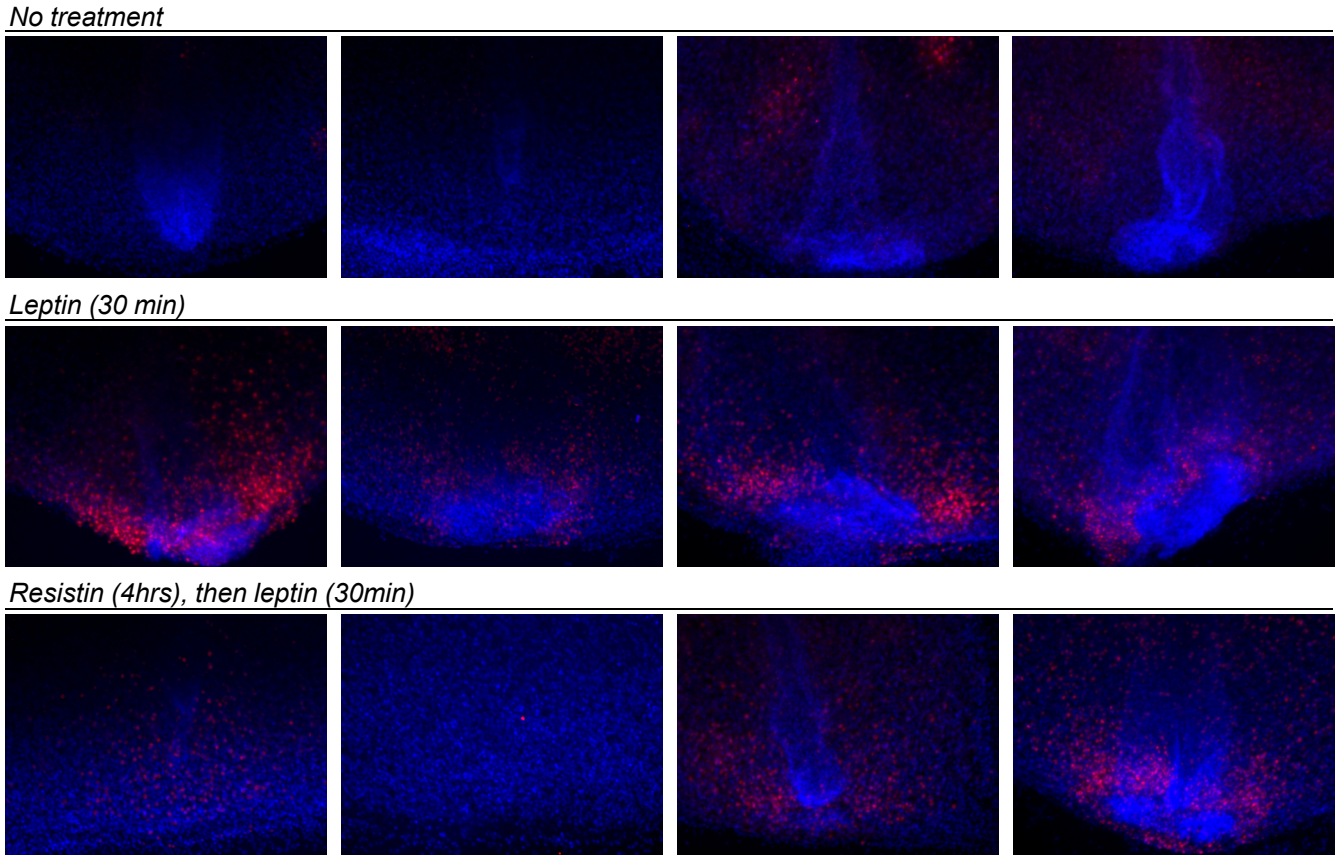

ESM FIGURE LEGENDS

ESM Figure 1: Male *Resistin*-Tg mice display some metabolic dysregulation comparable to their female counterparts. *Resistin*-Tg mice (black bars) exhibit (a) increased body weight (p=0.144), (b) normal glucose (p=0.898), (c) increased total % fat mass by NMR (p=0.133), (d) significantly increased leptin levels (p=0.026) on chow diet (WD increased both over baseline, (e) and elevated FA levels (p=0.213) as compared to wild type littermates (white bars). (f) Serum triacylglycerol levels and (g) liver weight are unchanged (p=0.678 and p=0.845, respectively), while (h) hepatic lipid levels were significantly reduced in male chow-fed *Resistin*-Tg mice as females on Western diet (p=0.020). (i) Triacylglycerol clearance was reduced in male *Resistin*-Tg mice on chow diet (p=0.035), but after the males were on Western diet for 5 weeks (j) the effect was lost (p=0.543). *p<0.05 compared to wild type. †p<0.05 with diet.

ESM Figure 2: Arterial plaques and lipid alterations in female *Ldlr*$^{-/-}$ *Resistin*-Tg mice. (a) No difference in atherosclerotic plaque quality and quantity between wildtype *Ldlr*$^{-/-}$ (white bars) and *Resistin*-Tg (black bars) females on *Ldlr*$^{-/-}$ background after 15 weeks on Western diet. (b) Slightly increased body weight *Ldlr*$^{-/-}$ *Resistin*-Tg females after 8 weeks on Western diet (p=0.018). (c) No difference in baseline serum triacylglycerol levels (p=0.172), but slightly impaired triacylglycerol clearance (d) in chow-fed *Ldlr*$^{-/-}$ *Resistin*-Tg females (AUC p=0.071). *p<0.05 compared to wild type *Ldlr*$^{-/-}$.

ESM Figure 3: Resistin overexpression reduced liver lipid content. (a) Reduced Western diet-induced gain of hepatic lipids in relation to weight gain in female *Ldlr*$^{-/-}$ *Resistin*-Tg mice (R^2=0.853; black bars) compared to *Ldlr*$^{-/-}$ wild type females (R2=0.390; white bars) . Reduced hepatic cholesterol (b) and triacylglycerol (c) levels in female *Ldlr*$^{-/-}$ *Resistin*-Tg mice after 15 weeks on Western diet (p=0.038 and 0.022). (d) No difference in hepatic VLDL- triacylglycerol production rate between female *Ldlr*$^{-/-}$ *Resistin*-Tg and littermate *Ldlr*$^{-/-}$ controls (p=0.080). *p<0.05 compared to wild type *Ldlr*$^{-/-}$.

ESM Figure 4: Brown adipose tissue and adipocyte phenotyping in *Resistin*-Tg mice. (a) Reduced UCP-1 immunofluorescence (green) in *Resistin*-Tg brown adipose tissue

(BAT) and increased lipid droplet size is not weight dependent (tissue from 35 g and 55 g matched mice shown). (b) Reduced UCP-1 protein levels in BAT of female Western diet-fed *Ldlr*$^{-/-}$ *Resistin*-Tg mice compared to littermate *Ldlr*$^{-/-}$ controls. Normal capacity for brown *ex vivo* adipogenesis isolated stromal-vascular fraction from *Resistin*-Tg BAT as judged by Oil-Red O stain (c) and normal mRNA levels of (d) *Fabp4*, *Cfd* and *Slc2a4*, while the expression of *Cidea*, *Ppargc1a*, *Pparg2*, and *Ucp1* are reduced (p=0.031, 0.050, 0.003, and 0.038) and *Cebpa* is increased (p=0.027) in differentiated primary *Resistin*-Tg brown adipocytes (black bars) compared to wild type (white bars). (e) Isoproterenol treatment (hashed bars) induced marked BAT gene expression in wildtype cells and significant increases in *Dio2* and *Ucp1* in *Resistin*-Tg cells (p=0.011 and p<0.001), but overall levels of response were less than wild type levels (each p<0.001). *p<0.05 compared to wild type. †p<0.05, †††p<0.001 with treatment.

ESM Figure 5: (a) Hypothalamic leptin-signaling gene expression in *Resistin*-Tg mice is reduced with *Cntf*, *Lepr*, and *Ptp1b* being the most different (p=0.075, p=0.097, and p=0.080, respectively). (b) Organotopic hypothalamic slices treated demonstrate reduced STAT3 phosphorylation (red) in the arcuate nucleus following leptin treatment if pre-treated with recombinant resistin protein. Slice size and thickness after 10 days of culture likely increase displayed variability. Blue=DAPI, third ventricle is centered in each image.

ESM METHODS

Generation of *Resistin* transgenic mice

The murine *Resistin* coding sequence was amplified from a fetal mouse cDNA library and cloned into pCR4TA (Invitrogen). This was subcloned into a transgenic vector under the control of 5.4 kb aP2 promoter. A rabbit beta globin 3'UTR was engineered following the resistin gene. The final 8.5 kb fragment containing the aP2 promoter, *Resistin* gene and 3'UTR was sequenced for verification and the linearized by HindIII and SacII digestion. The purified DNA was submitted for pro-nuclear injection into pure FVB embryos. Genotyping primers F (GCCA CCAT GAA GAA CCT TTC ATT TCC CCT C) and R (GGA TCC TCA GGA AGC GAC CTG CAG CTT AC) yielded a 350 bp product. Transgene positive lines were subsequently backcrossed to a pure C57/B6 background or C57/B6-backgroun *Ldlr*$^{-/-}$ mice for minimally 10 generations with regularly pure C57/B6 maintenance

Blood biochemistry

Insulin, leptin and adiponectin were measured by commercial ELISA kits (Millipore, USA). Resistin levels were measured by commercial RIA kit (Millipore, USA). Glucose concentrations were determined with Sigma Diagnostics Glucose Reagents and fatty acid levels were measured with NEFA-HR(2) (Wako Pure Chemical Industries, Japan). Triacylglycerol and cholesterol were measured with Infinity reagent (Thermo Scientific, USA). The cholesterol and triacylglycerol content of lipoprotein fractions in the plasma were determined following fast-performance liquid chromatography (FPLC) separation.

Oil red O stain of aortic root sections and livers

The tissues were fixed by 4% paraformaldehyde (perfusion and immersion) for 20-24 hours, cryoprotected with sequential 10% and 18% sucrose equilibrations for 12-hours-each at 4°C, and then cryo-embedded in optimal cutting temperature medium (OCT, Sakura Finetek, USA). Multiple plane 8μm thickness cryostat sections were prepared of each tissue and temporarily stored at -80°C. Staining for lipids

with Oil Red-O was conducted according to established histologic protocol. Quantification of Oil-Red-O stain positive areas was performed by ImageJ software with each image blindly thresholded for neutral lipid stain.

Immunohistochemistry of aortic root sections

The tissues were fixed by 4% paraformaldehyde (perfusion and immersion) and embedded in paraffin for immunohistochemical analysis of Mac2 (rat anti-mouse Mac2, Cedarlane, USA) and CD163 (rabbit anti-mouse CD163, Santa Cruz Biotechnology, USA). Endogenous peroxidase activity was blocked by Dual Endogenous Enzyme Block (Dako, USA). Detection was performed by Liquid DAB+ Substrate Chromogen System, using secondary anti-rat or anti-rabbit biotinylated antibodies and HRP-streptavidin (all reagents from Dako, USA).

Hepatic Steatosis measurements:

Mice were anesthetized with isoflurane and a CT-scan was performed at a resolution of 93µm using the short scan mode (180°) on a eXplore Locus *in vivo* MicroCT Scanner from GE Healthcare. Liver lipid content was estimated by obtaining the average CT-value in multiple regions well within the liver, as validated previously [1].

Lipids were extracted from 100-200 mg liver tissue pieces according to the Folch method [1]. The chloroform phase was brought up to 5 mL and triplicates of 50 ml together with standards were dried down by the addition of 10 ml of a 2:1 chloroform triton mix. Tracylglycerol levels were measured with Infinity reagent (Thermo Fisher, USA). Sphingolipid analysis was performed by LC-MS/MS as previously described [2].

#

Western blot

Brown adipose tissue was carefully dissected and snap-frozen in N_2(l) and stored at -80°C until analysis. The tissues were homogenized in ice-cold TBS pH 7.4 1% Triton supplemented with protease inhibitor cocktail. The tissue homogenates were agitated for 1h at 4 °C, extracts were cleared at 20,000 x g

for 20 minutes at 4°C and total protein concentration were measured with BCA Protein Assay Kit (Pierce Protein Research Products, Thermo Scientific, USA). Equal amounts of protein were mixed with 5x Laemmli sample buffer, resolved on respectively 12% Tris-Glycine gels (BIO-RAD), followed by transfer to PVDF membrane (Millipore, USA). Blots were probed with rabbit anti-mouse UCP-1 antibody (Abcam, USA). Bound antibodies were detected with IRDye800-conjugated anti-rabbit secondary antibodies (Rockland). Membranes were scanned with the LI-COR Odyssey infrared imaging system.

Quantitative real-time RT-PCR

Tissues were collected in RNAlater (Ambion, USA) and stored at -80°C until Trizol reagent (Invitrogen, USA) extraction followed by RNA purification using RNeasy Mini Kit and RNase-Free DNase (Qiagen, USA). RNA was reverse transcribed to cDNA by iScript cDNA synthesis kit (Bio-Rad, USA); Power SYBER Green PCR Master Mix (Applied Biosystems) was used for the quantitative PCR reactions on hypothalamic cDNA while IQ SYBR Green Supermix (Bio-Rad) was used for all other tissues. *Actb* was universally used as an endogenous control. Primer sequences used are indicated in **ESM Table 1**.

Leptin Treatment

To measure leptin-induced weight loss, 5 mice per group were fasted for 4hrs (starting at 10 am) before leptin injections. 5μg/g body weight leptin was injected intraperitoneally for 7 days to HFD mice and 2 μg/g body weight leptin was used for normal chow-fed mice. Weight loss was measured throughout. To assess leptin-induced STAT3 phosphorylation directly in the hypothalamus, 16 mice were prepared for intra-third cerebral ventricle (ICV) injection of leptin by implantation with short pedestal cannula systems (Plastics One Inc., Roanoke, VA) under isofluorane. After one week of recover, mice were fasted for 16 hours and injected with 1 μl of 0.05 μg/μl or PBS control [3, 4]. Mice were perfusion fixed with 4% paraformaldehyde 30 minutes following ICV injection.

#

Organotypic hypothalamic culture

Organotypic brain slices were obtained from 16 young male wildtype mice as previously described [5]. Briefly, brains of 10-12 day old mice were quickly removed and sectioned at a thickness of 250 μm (3-4 slices per mouse). Coronal slices containing the arcuate nucleus were placed on 0.4μm pore Millicell-CM filters (Millipore), and then maintained at an air-media interface in MEM based medium (MEM with 25% horse serum, 25% HBSS, 1% glutamax, 0.5% D-glucose) for 10 days. Slices were changed to 2.5% horse serum medium overnight prior to the experiment. Subsequent slices were incubated with the addition of resistin (100 nmol/l final concentration; purified from stably transfected 293T cells as previously [6]) or PBS for 4 hours followed by the presence or absence of leptin (100 nmol/l; Peprotech, Rocky Hill, NJ) for 30 minutes.

Hypothalamic pSTAT3 measurement

STAT3 phosphorylation was assessed on organotypic hypothalamic slices by immunofluorescence (rabbit anti-pSTAT3; Cell Signaling); anti-rabbit Alexa594 was visualized and imaged in conjunction with DAPI-labeled nuclei on a Zeiss AxioObserver microscope. Images were captured as z-stacks using a 1.57 μm increment and equivalent exposure times throughout the tissue slice; these series were maximally projected using Zeiss AxioVision 4.7 software and pSTAT3+ area was measured using Image J thresholded %area. 10-μm thick serial sections were prepared from fixed hypothalami and similarly labeled and imaged as above. pSTAT3 area in the arcuate nucleus was averaged across 3-6 serial sections (in which the arcuate nucleus was clearly defined) to obtain the value for each mouse.

#

Primary Brown Adipocyte Differentiation and Culture

Brown adipose tissue from two mice of each group (aged 6 weeks old) was carefully dissected, minced, and digested in buffer containing 123 mmol/l NaCl, 5 mmol/l KCl, 1.3 mmol/l $CaCl_2$, 5 mmol/l glucose, 100 mmol/l HEPES, 4% BSA, and 1.5 mg/ml Collagenase B (Roche) for 45 minutes. Filtered digests were spun at 600 x g for 5 minutes and pelleted SVF cells were resuspended in 20% FBS high glucose DMEM containing 20 mmol/l HEPES and cultured on collagen-coated tissue culture plates. Media

was changed daily to remove non-adherent cells and debris. After two passages, cells were plated at equal density for differentiation assays. Adipocyte differentiation was induced as previously described [7]. Confluent cells were treated for 48 hr in medium containing 10% FBS, 0.5 mmol/l isobutylmethylxanthine, 125 nmol/l indomethacin, 1 µmol/l dexamethasone, 20 nmol/l insulin, 1 nmol/l T_3, and 1 µmol/l rosiglitazone (Cayman Chemical, Ann arbor, MI). Two days after induction, cells were switched to maintenance medium containing 10% FBS, 20 nmol/l insulin, 1 nmol/l T_3, 1 µmol/l rosiglitazone. Oil Red-O staining of triplicate wells was performed as previously described [8]. Isoproterenol (10 µmol/l; Sigma) was added to media for 4-hours before RNA extraction in functional studies. RNA was extracted, reverse transcribed, and analyzed as above.

ESM METHODS REFERENCES

1. Asterholm, I.W. and P.E. Scherer, *Enhanced metabolic flexibility associated with elevated adiponectin levels.* Am J Pathol, 2010. **176**(3): p. 1364-76.
2. Holland, W.L., et al., *An FGF21-adiponectin-ceramide axis controls energy expenditure and insulin action in mice.* Cell Metab, 2013. **17**(5): p. 790-7.
3. Faouzi, M., et al., *Differential accessibility of circulating leptin to individual hypothalamic sites.* Endocrinology, 2007. **148**(11): p. 5414-23.
4. Scott, M.M., et al., *Leptin targets in the mouse brain.* J Comp Neurol, 2009. **514**(5): p. 518-32.
5. Fukuda, M., et al., *Monitoring FoxO1 localization in chemically identified neurons.* J Neurosci, 2008. **28**(50): p. 13640-8.
6. Rajala, M.W., et al., *Adipose-derived resistin and gut-derived resistin-like molecule-beta selectively impair insulin action on glucose production.* J Clin Invest, 2003. **111**(2): p. 225-30.
7. Rajakumari, S., et al., *EBF2 determines and maintains brown adipocyte identity.* Cell Metab, 2013. **17**(4): p. 562-74.
8. Gupta, R.K., et al., *Transcriptional control of preadipocyte determination by Zfp423.* Nature, 2010. **464**(7288): p. 619-23.

Gene	Forward	Reverse
Adipoq	TGGGGACCACAATGGACTCTA	TGGGCTATGGGTAGTTGCAGT
Cfd	GCGATGGTATGATGTGCAGAG	CAACGAGGCATTCTGGGATAG
Cebpa	CAAGAACAGCAACGAGTACCG	GTCACTGGTCAACTCCAGCAC
Cidea	TCCTATGCTGCACAGATGACG	TGCTCTTCTGTATCGCCCAGT
Dio2	CATTGATGAGGCTCACCCTTC	GGTTCCGGTGCTTCTTAACCT
Elovl3	GTGTGCTTTGCCATCTACACG	CTCCCAGTTCAACAACCTTGC
Fabp4	ACAGCTCCTCCTCGAAGGTTT	AAGCCCACTCCCACTTCTTTC
Lpl	GAGCCAAGAGAAGCAGCAAGA	GAGAAATCTCGAAGGCCTGGT
Ppargc1a	GCACCAGAAAACAGCTCCAAG	CGTCAAACACAGCTTGACAGG
Pparg1	TGAAAGAAGCGGTGAACCACTG	TGGCATCTCTGTGTCAACCATG
Pparg2	GCATGGTGCCTTCGCTGA	TGGCATCTCTGTGTCAACCATG
Prdm16	ACACGCAGTTCTCCAACCTGT	CCCACAGTCCTTGCACTTGAT
Rps18	CATGCAGAACCCACGACAGTA	CCTCACGCAGCTTGTTGTCTA
Slc2a4	ACATACCTGACAGGGCAAGGA	CTTTCGGGTTTAGCACCCTTC
Ucp1	TCTCAGCCGGCTTAATGACTG	GGCTTGCATTCTGACCTTCAC
Actb	TGGCATTGTTACCAACTGGG	GGGTCATCTTTTCACGGTTG
Cntf	AGGGGCCTAGTTTTCTCAGC	GGGTCAACCCTACTTGACGA
Epac	TCTGTCTCTGCCCTGTTCCT	CCGCAAAGAAAGAGTTGAGG
Lepr	GGGAATGAGCAAGGTCAAAA	TCAAGTCCCCTTTCATCCAG
Ptpn1	ATGTCAGCCCTTTTGACCAC	GAAGTGCCCACATGTGTTTG
Socs3	ATTCACCCAGGTGGCTACAG	GCCAATGTCTTCCCAGTGTT
Stat3	TCACTTGGGTGGAAAAGGAC	TGGTCGCATCCATGATCTTA

ESM Table 1: Primer pairs utilized in this study for quantitative PCR analyses.